

Reproductive Barriers as a Byproduct of Gene Network Evolution

Chia-Hung Yang¹ and Samuel V. Scarpino^{1,2,3,4,5*}

*For correspondence:
s.scarpino@northeastern.edu

¹Network Science Institute, Northeastern University, Boston, United States; ²Department of Marine and Environmental Sciences, Northeastern University, Boston, United States; ³Department of Physics, Northeastern University, Boston, United States; ⁴Department of Health Science, Northeastern University, Boston, United States; ⁵ISI Foundation, Turin, Italy

Abstract Speciation in the absence of divergent selection remains a topic of active debate in evolutionary biology. Existing empirical and theoretical studies have linked the process of speciation to complex genetic interactions. Gene Regulatory Networks (GRNs) capture the inter-dependencies of gene expression and encode information for individual development on a molecular level, which form a feedback loop to learn both patterns and effects of hybrid incompatibilities. Here, we develop a pathway framework considers GRNs as a functional representation of coding sequences. We then simulated the dynamics of GRNs through a simple model integrating natural selection, genetic drift and sexual reproduction and uncovered reproductive barriers among allopatric population subjected to identical selection pressure. A minimal mechanism of how reproductive isolation emerged was identified by numerical counter-factual analyses. We discuss how many features of our results are able to account for observed empirical patterns, which are currently in opposition to classical models of speciation. This study adds support for the central role of gene networks in speciation and their potential to shed light on as yet largely unexplained patterns in evolution.

Introduction

Over the past 100 years, the role of reproductive isolation due to genetic differences between populations has received considerable attention in both the empirical and theoretical literature on speciation (*Rieseberg et al., 1996; Coyne and Allen Orr, 1998; Marques et al., 2019; Satokangas et al., 2020*). Through this work, it is widely accepted that divergent selection between geographically isolated populations can facilitate speciation due to the accumulation of genetic incompatibilities (*Bateson, 1909; Dobzhansky, 1936; Muller, 1942*). Despite well-established examples from *Drosophila* (*Brideau et al., 2006*), *Xiphophorus* (*Wittbrodt et al., 1989; Powell et al., 2020*), *Oryza* (*Yamamoto et al., 2010*), *Arabidopsis* (*Bikard et al., 2009*), and *Mus* (*Davies et al., 2016*), the genetics and evolutionary history of incompatibilities are typically far more complex than suggested by early models (*Marques et al., 2019*).

Classically post-zygotic, genetic isolation is thought to arise due to epistatic interaction between loci, where alleles arise and fix in allopatry prior to secondary contact, i.e., the Bateson-Dobzhansky-Muller (BDM) model (*Bateson, 1909; Dobzhansky, 1936; Muller, 1942*). However, many incompatibilities uncovered using high-throughput molecular analyses (*Kuzmin et al., 2018*) and quantitative traits loci mapping (*Turner et al., 2014; Chae et al., 2014*), do not conform to the processes suggested by BDM model. In particular, in both natural populations and model organisms, studies have found reproductive barriers exist between allopatric populations experiencing similar selection

43 pressures (*Schluter, 2009*) and many of the alleles underlying genetic incompatibility predate the
44 allopatric split of populations (*Marques et al., 2019*). Both of which are clear violations of the BDM
45 model. As a result, why and how genetic incompatibilities arise without divergent selection and
46 involve alleles that pre-date the allopatric separation of populations remains one of the most
47 profound questions in evolutionary biology *Marques et al. (2019)*.

48 Analytical and computational models have proposed theoretical explanations for the observed
49 patterns of complex genetic interaction underlying post-zygotic isolation. A collection of models
50 considered *de-novo* allele substitutions on the population level and the accompanying accumulation
51 of hybrid incompatibilities. For example, *Orr (1995)* predicted that the number of incompatibilities
52 should increase faster than linearly with the number of substitutions. The study by *Orr* also
53 suggested higher prevalence of complex genetic interactions than simple pairwise incompatibilities.
54 This so-called "snowballing" effect has been further extended by incorporating protein-protein
55 interaction and RNA folding (*Livingstone et al., 2012; Kalirad and Azevedo, 2017*).

56 The substitution-based approaches nevertheless are largely incompatible with emerging data
57 on the evolutionary history of alleles involved in reproductive isolation (*Marques et al., 2019*). In
58 addition, many models make an implicit assumption that two allopatric lineages only differed by
59 fixed alleles, which does not capture the empirical diversity among individuals' gene expression in
60 natural populations (*Gould et al., 2018*). More importantly, substitutions originating from *de-novo*
61 mutations fail to explain the recent evidence that ancient alleles underlying reproductive barriers
62 often predate speciation events (*Sicard et al., 2015; Meier et al., 2017; Nelson and Cresko, 2018;*
63 *Wang et al., 2019; Duranton et al., 2019; Marques et al., 2019*).

64 Another class of computational approaches focused on the overall regulation structure that is po-
65 tentially accountable for complex genetic interactions, whose evolution then creates a feedback loop
66 to generate hybrid incompatibilities. Gene regulatory networks (GRNs) describe inter-dependencies
67 between gene expression and encode information of individual development on the molecular level.
68 *Johnson and Porter (2000)* simulated a single linear regulatory pathway as a sequence of matching
69 functions for binding sites, which resulted in reduced hybrid fitness compared to non-epistatic
70 models. *Palmer and Feldman (2009)* explored the developmental process where the expression of
71 gene products was iteratively determined through the regulatory networks. Diverse dynamics of
72 hybrid incompatibilities was revealed which suggested the role of neutral gene regulatory evolution
73 on speciation. Recently, *Schiffman and Ralph (2018)* modeled gene networks as linear control
74 systems and demonstrated that reproductive isolation can be a consequence of parallel evolution
75 of GRNs with equivalent mechanism.

76 The implications from gene network evolution are not mere outcomes of incorporating complex-
77 ity into existing computational models. Instead, it is natural to consider GRNs to study evolutionary
78 processes due to their close relation to coding sequences. Ideally, and hypothetically given "omni-
79 science" over the genomes including comprehension of every fundamental interaction between
80 molecules, one can reconstruct inter-dependencies among genes and thus obtain the GRN from a
81 bottom-up approach. Of course, this ambition is far from practical and even sounds like a fantasy.
82 Yet, it shows that GRNs are essentially a direct abstraction of the genome sequence. Furthermore,
83 this abstraction has been proposed as the heart of the omnigenic perspective of complex traits
84 (*Boyle et al., 2017*), which aims to ultimately map genotypes to phenotypes. GRNs therefore bridge
85 the gap between inheritance factors and physiological traits, whose dynamics over generations
86 then becomes a candidate to understand speciation.

87 Moving beyond substitution-based approaches, models that consider the evolution of GRNs are
88 more flexible and can embrace recent observations such as the rich genetic variation in natural
89 populations and the that incompatible alleles often far predate speciation events. That modern
90 genetic details on incompatibilities are often opposed to existing theory is well articulated by
91 *Marques et al. (2019)* who suggested that these two lines of empirical evidence can be consolidated
92 into a "combinatorial view" of speciation. The combinatorial mechanism proposes that, if there
93 was a past admixture event or if standing genetic variation persists, the reassembly of these old

94 genetic variants can facilitate rapid speciation and adaptive radiation. Here, we integrate the
95 combinatorial view and the evolution of GRNs. Specifically, we study the inherited molecular
96 pathways encoded in GRNs, which are established upon genetic elements and propagate chemical
97 signals that produce physiological traits. These pathways amplify a gene networks' potential to
98 disentangle the genotype-phenotype map in light of epistasis.

99 Specifically, we propose a pathway framework for studying the evolution of genetic interactions
100 that considers GRNs as a functional representations of coding sequences. The pathway framework
101 takes a network-science approach to model how a current generation's GRNs bring forth the
102 next generation's GRNs. Presuming ancestral variation as in the combinatorial view of speciation,
103 the dynamics of individuals' gene networks was simulated through a naive model integrating
104 independent assortment during sexual reproduction, genetic drift resulting from finite population
105 size and natural selection on gene network functionality. We observed emergence of reproductive
106 barriers among allopatric populations under identical selection pressure, where early evolutionary
107 divergence between lineages was critical for barriers to arise. We concluded that it was the
108 functional degeneracy nature of GRNs that accommodated potential lethal pathways in a diverse
109 genetic background and led to reproductive barriers.

110 Results

111 The Pathway Framework: Networks as a Functional Representation of Genetic Interactions

112 Gene interactions networks are conventionally built such that genes are "nodes" and interactions
113 between genes are "edges" or links, for examples see *Tong et al. (2004)*; *Schlitt and Brazma (2007)*;
114 *Langfelder and Horvath (2008)*. Here we propose an alternative methodology, termed the *pathway*
115 *framework*, for constructing gene interaction networks. The key idea is to conceptualize genes,
116 or alleles of genes, as "black boxes" that describe their expression behavior. More precisely, the
117 pathway framework transforms alleles of genes into directed edges pointing from nodes that are
118 activator/repressor molecules, e.g., transcription factors, and nodes that represent gene products,
119 e.g., proteins. For example, in *Figure 1* we show how: a.) a gene is activated by a transcription
120 factor and generates a protein product (top-right), b.) two genes interact via a transcription
121 factor created by one gene that activates the other (middle-right), and c.) genes can interact via
122 shared transcription factors (bottom-right). As a result of its flexibility, arbitrarily complex genetic
123 interactions can be encoded as "pathways" through a gene interaction network.

124 Importantly, while our proposed representation is closely related to conventional gene interac-
125 tion networks (and a direct mapping between the two always exists when considering interactions
126 mediated by a single class of molecules, e.g., proteins), the pathway framework is often either a
127 more compact or informative representation. For example, anytime a gene is regulated by a protein
128 product from another gene, the conventional framework usually show redundancy that does not
129 appear in the pathway framework, and the pathway framework will capture information not present
130 in the conventional construction, e.g., see Box 1. Because the computational complexity of network
131 analyses often scales non-linearly with the number of edges, switching to the pathway framework
132 can facilitate a more robust exploration of model space.

133 The pathway framework further highlights how phenotypes are a product of both genetics and
134 the environment (not all nodes in the pathway framework need be gene products). Concentrating
135 on the molecular basis of physiological traits, a phenotype can be thought of as the biochemical
136 status of a universal collection of nodes in the pathway framework, e.g., gene products such as
137 proteins or environmental stimuli. Therefore, under the pathway framework, the development of a
138 phenotype can be viewed as an iterative process of chemical signals propagating through woven
139 pathways built from a groups of "inherited metabolisms", namely the functionality of genes, and
140 external signals from the environment. As a result, the pathway framework can readily capture
141 genetic, environment, and gene x environment effects in the same network.
142

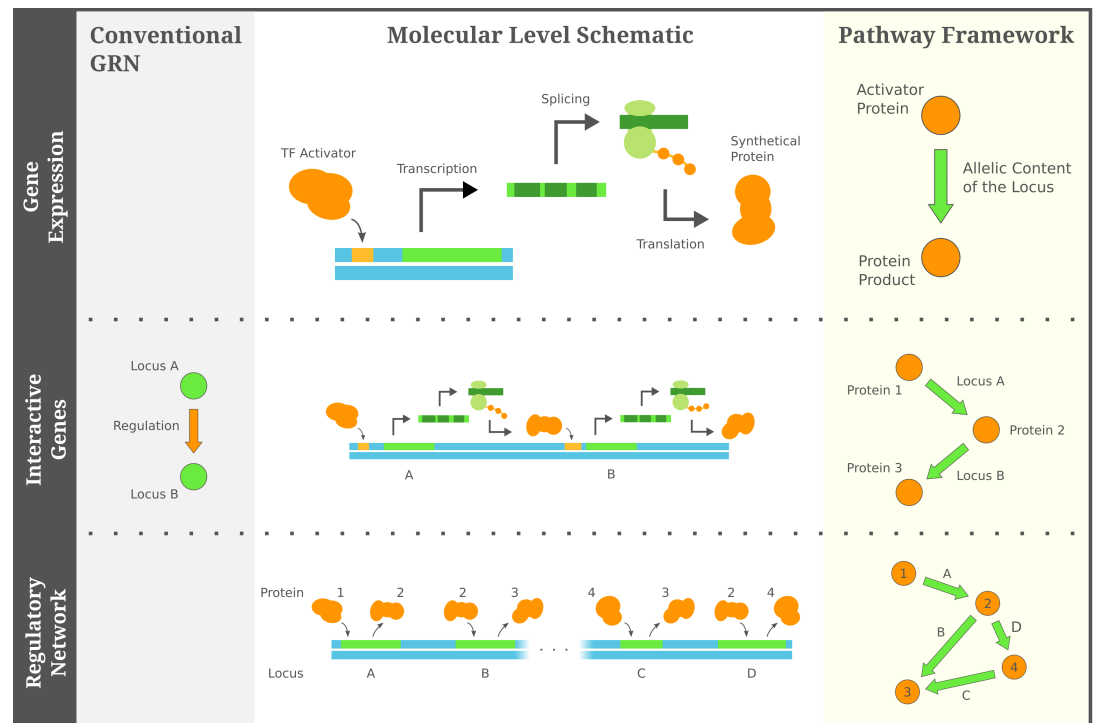


Figure 1. Pathway framework captures complex genetic interactions through consecutive regulatory pathways. In contrast to directly representing genetic interactions as in conventional GRN, the pathway framework abstracts genes as black boxes of their expression behavior. It turns alleles of genes into edges between the transcription factors and the protein products, and regulatory interactions between genes are encapsulated by consecutive pathways.

144

Box 1. Pathway framework is often a more compact representation

145

146

147

148

149

150

151

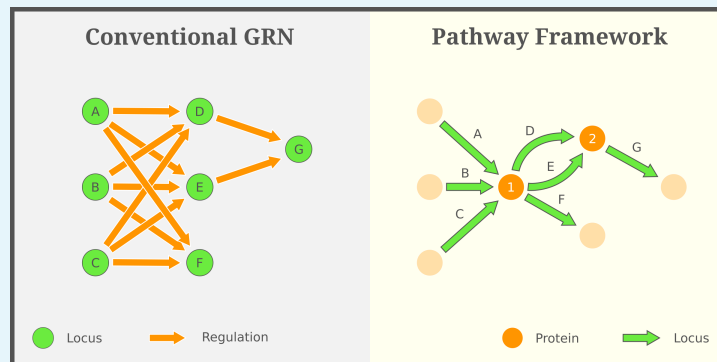
152

153

154

The pathway framework is usually more informative than the conventional construction of GRNs since it directly shows the expression behavior of genes. When considering genetic interactions that are mediated by a single class of molecules, e.g., one gene being regulated by the protein product of another, the pathway framework takes advantages of this information and presents genetic interactions in a compact pathway format. On the contrary, a conventional GRN lacks the specific regulatory context, and thus it has to present all pairs of interacting genes as individual edges rather than summarizing them by a smaller set of protein mediators. More technically, the pathway framework and a conventional GRN correspond to the first- and second-order de Bruijn graph (*De Bruijn, 1946*) respectively, and higher-order de Bruijn graphs usually tackle combinatorial problems at the cost of introducing redundant elements.

155



156 **Evolutionary Mechanisms under the Pathway Framework**

157 Although in its most abstract state, the pathway framework can include nodes that are not proteins
158 and not directly involved in gene regulation, we focus here on the evolution of GRNs where all nodes
159 are proteins directly involved in transcriptional regulation. To model and simulate the evolution of
160 GRNs, the pathway framework translates evolutionary mechanisms, such as mutation, independent
161 assortment, recombination, and gene duplication, into graphical operations on the gene networks¹.
162 Because mutation of a locus can potentially alter its protein product and/or the transcription
163 factor binding region(s), we consider mutation as rewiring process where the incoming and/or
164 outgoing directed edges are re-directed to point from or to different nodes (**Figure 2**, top-right).
165 Independent assortment during meiosis can be modeled via edge-mixing of parental GRNs such
166 that an offspring acquires alleles, i.e., edges in the GRN, from both parents (**Figure 2**, bottom).
167 Similar to mutation, recombination is an edge-rewiring process that is constrained to swapping
168 binding sites or transcription factors at the same locus. Finally, gene duplication is equivalent to
169 adding a parallel edge that represents the identical allelic content of a duplicated locus.

170 An individual's viability subjected to natural selection is a response to the molecular phenotypic
171 status, which, under the pathway framework, can be modeled as a fitness function associated with
172 the collective state of nodes in the gene network. For example, one could study the time-varying
173 concentration of each protein, attach a continuous dynamic or a stochastic reaction to every allele
174 and define fitness as a function of the high-dimensional concentration vector, etc.. On the other
175 extreme, we instead consider Boolean networks, which have been shown to effectively portray
176 many of the relevant dynamical features of empirical regulatory systems (**Davidich and Bornholdt,**
177 **2008**). In this minimal scenario, each protein is assigned to a Boolean state — present or absent.
178 External environmental signals stimulate the existence of some proteins in the organism. The
179 logical states then cascade through the genetic pathways, where given the presence of a gene's
180 transcription factor, its allele turns on and generates a protein product. The phenotype of a GRN is
181 thus the "reachability" from the environmental stimuli, whose binary survival is defined via a sharp
182 fitness landscape over plausible collective Boolean states (**Figure 2**, top-left).

183 We further adopt the Boolean-state assumption of GRNs because it readily sheds light on the
184 formation of hybrid incompatibilities. A hybrid incompatibility is a combination of alleles that
185 were separated in parental lineages but are present in hybrids and cause fatalities. Moreover, the
186 combination is minimal in the sense that the lack of any of its allelic elements will not lead to an
187 inviable hybrid. In the pathway framework, suppose that the binary viability only depends on a set
188 of lethal proteins, i.e. an individual will not survive selection if any of those protein are present, a
189 combination of alleles that includes a pathway from a environmental stimulus to a lethal protein
190 makes the GRN inviable. If the alleles exactly comprise a simple path, which contains no cycles,
191 they become a minimal combination and thus form an incompatibility. Additionally, The complexity
192 of genetic interactions can be characterized by the number of alleles involved, which is called the
193 order of hybrid incompatibility and related to the length of the simple pathway².

194 **Simulating the Evolution of GRNs**

195 Briefly, we first consider a Wright-Fisher model of evolution with natural selection, i.e., constant
196 population size, no mutation, no migration, non-overlapping generations, and random mating.
197 Selection occurs during the haploid stage of the life-cycle, which fuse randomly after selection,
198 i.e., create diploids, and undergo meiosis to generate the subsequent generation (simulations are
199 further detailed in the **Methods**). Populations are seeded such that each individual has a randomly
200 generated GRN and evolve until a single GRN fixes in the population.

201 **Figure 3a** shows the proportion of individuals in the population that survive natural selection.

¹These graphical operations particularly focus on edges in the GRNs, while remaining the underlying node set constant because the nodes represent all *possibly existing* proteins in the organism.

²Since for $n \geq 1$, $n + 1$ alleles form an n th-order incompatibility, the order of genetic interaction is then the path length minus one.

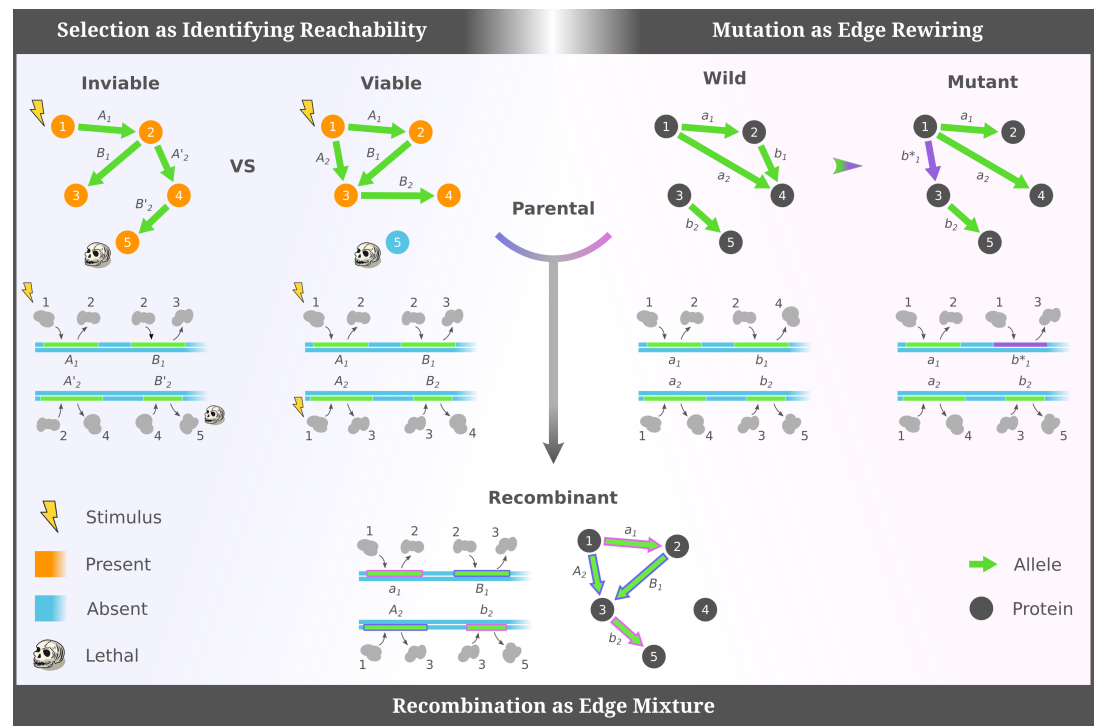


Figure 2. Pathway framework turns evolutionary mechanisms into graphical operations on the GRNs. Since the pathway framework directly models the functionality of alleles of genes as edges, mutation and recombination can be modeled as edge-rewiring and edge-mixing respectively, while a minimal selection scenario of binary fitness can be modeled as identifying reachability in the GRNs.

202 Initially, the fraction of viable individuals differed dramatically between simulations with different
 203 initial conditions due to the variation of randomly seeded GRNs. As the gene networks evolved,
 204 the population's viability increased and quickly reaches a state where every individual survives
 205 selection (dashed line). During this 100% survival stage, natural selection was no longer effective
 206 and the population evolves to fixation via genetic drift. Not surprisingly, our results demonstrate
 207 that GRNs can rapidly evolve from a heterogeneous population with low average viability to "match"
 208 and imposed environment.

209 In addition to achieving 100% survival, populations always fix for a single GRN. **Figure 3b** plots
 210 the number of structurally-distinct GRNs in each generation. The decreasing trend demonstrates
 211 that, although various GRNs have equal survival probability, it became more and more likely that
 212 individuals shared a common GRN. Moreover, the populations always fixed a single GRN (dotted
 213 line) after a sufficiently long period of time. This phenomenon can be intuitively explained by
 214 the mechanism of sexual reproduction. In our model, parents with identical GRN would lead to
 215 offspring of the same GRN, since any two corresponding groups of segregated alleles retrieved the
 216 parental gene network. Thus once there was a majority gene network in the population, it has a
 217 higher chance to retain its genetic configuration in the next generation rather than being replaced
 218 by shuffled variants.

219 Lastly, to better understand how parallel lineages evolve, we consider a scenario where mul-
 220 tiple allopatric populations are seeded with the *same* initial conditions. Similarly, each allopatric
 221 population rapidly achieves 100% survival and then fixes a single GRN. However, across allopatric
 222 populations, seeded from the same initial conditions, many different GRNs fixed. **Figure 4** presents
 223 the distribution of fixed GRNs for a smaller-scale simulation (Setup 2 in Methods). We see that the
 224 fixed gene networks were diverse and non-uniformly distributed. Despite being under identical
 225 selection forces and having the same initial condition, lineages evolving from a common ancestral
 226 population fixed alternative GRNs. This result demonstrates that a broad range of GRNs can survive

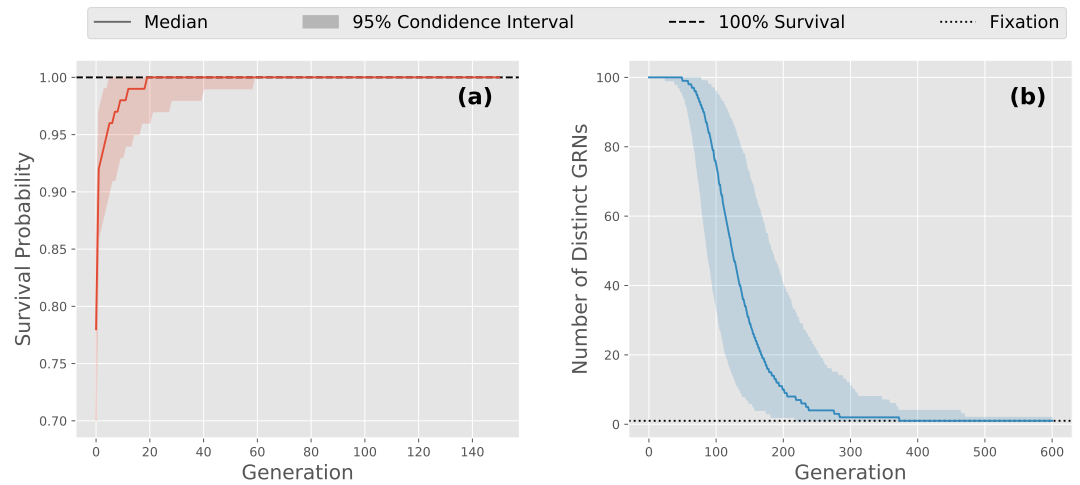


Figure 3. Populations adapted to the environment and then fixed a single GRN. Here we show, for every generation of GRN evolution across multiple allopatric populations with different initial conditions: **(a)** the survival probability of an individual and **(b)** the number distinct GRNs in each population, where two individuals' GRNs were deemed effectively identical if they were isomorphic. The average viability of each population increased over time and rapidly achieved 100% survival, which indicates that evolution of GRNs drove adaptation toward the imposed environment. We also observe decreased variation of GRNs as they evolved, with individuals in the same allopatric population, i.e., simulation run, eventually fixing for the same GRN.

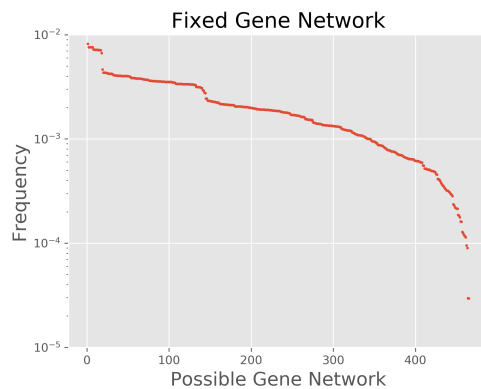


Figure 4. Fixation of parallel lineages resulted in a wide range of GRN structures. We simulated isolated populations from the same initial conditions until they reached fixation. In this case Setup 2 in Methods was applied in order to tractably enumerate all plausible GRN, and the ancestral populations were chosen such that the fixation was unbiased by the initial allele frequencies. The 10^7 acquired GRNs were categorized into 465 viable structures and the fixation frequency of each structure was plotted in a descending order. The distribution shows that isolated lineages fixed alternative gene networks, some among which were more favorable under our model of GRN evolution.

227 the given selection pressure. Furthermore, none of the viable GRN structures had a zero fixation
 228 probability, indicating an thorough exploration of evolution in the space of possible GRNs. That so
 229 many different GRNs fixed suggests that evolution was less governed by a definite trajectory, but
 230 instead it occurs via an uncertain realization among all the possibilities constrained by the ancestral
 231 population and the selection pressure.

232 Reproductive Barriers Arose Rapidly as Gene Networks Evolved

233 If the survival probability and fitness of GRNs were identical, the distribution of fixed networks
 234 should be uniform over all viable conformations. Because we observe a strongly non-uniform
 235 distribution (see *Figure 4*) some other form of selection is likely operating on the GRNs. We note
 236 that during random mating, even between two parents with viable GRNs, some of their shuffled
 237 offspring can be inviable. Coupled with the observation that different allopatric populations, i.e.,
 238 simulation runs, fix alternative GRNs from the same initial conditions, we hypothesized that some
 239 degree of reproductive isolation may exist between these fixed populations.

240 To test for the presence of reproductive isolation, we performed a "hybridization" experiment
 241 between parallel lineages that had reached fixation. Starting with lineages branched from a

242 common ancestral population, two fixed lineages were randomly selected and interbred. Hybrids
243 were generated and the reproductive isolation metric (RI) between the parental populations was
244 computed (see *Methods*). By repeating this procedure, we obtained a distribution of reproductive
245 isolation, as demonstrated in *Figure 5a* inset. Despite a large fraction of crosses resulting in nearly
246 zero RI, we discovered pairs of lineages with positive reproductive isolation metric. Specifically,
247 the RI distribution displays several regions of positive reproductive isolation such that a high
248 percentage of hybrid offspring are inviable. Thus, we conclude that reproductive barriers between
249 fixed lineages, derived from the same initial population and experiencing identical selection, exist.

250 Given noticeable reproductive barriers between fixed lineages, we further studied when those
251 barriers first manifested during GRN evolution. Note that because our simulations did not contain
252 mutation, incompatibilities arise because of shuffling during meiosis. Here, instead of waiting until
253 GRN fixation, we instead evolve lineages for T generations and then cross them to generate hybrids
254 as described above. By varying T , a series of reproductive isolation distributions were acquired.
255 *Figure 5a* collects and displays them in a heat map. A vertical slice represents a RI distribution as
256 in the inset panel, but crosses were made after T generations rather than waiting for lineages to
257 reach fixation. We see that the regions of high incompatibility noted in *Figure 5a* inset becomes
258 bands in the heat map, which allows us to trace the emergence of reproductive barriers.

259 Initially the reproductive isolation distribution was relatively symmetric around zero. However,
260 As GRNs evolved, the range of RI broadened and its extreme value in the positive tail increased.
261 The trend towards higher levels of RI decelerated after 100 generations; it then stabilized and
262 formed a band structure, where crosses cluster around certain levels of reproductive isolation.
263 *Figure 5a* hence reflects that reproductive barriers existed at low levels as soon as the lineages
264 started evolving independently and peaked at a time prior to GRN fixation. By assumption, the
265 alleles underlying RI were present in the ancestral population, but we further conclude that RI
266 peaked well before fixation of GRNs.

267 Next, for incompatible hybrids generated in our crossing experiment, we determine how complex
268 the underlying mechanism of RI was. Specifically, *Figure 5b* shows how frequently an inviable hybrid
269 resulted from an incompatibility of a certain order. We see that hybrid incompatibilities spanned
270 over a broad range of interaction orders. Importantly, the simple two-allele interaction was only
271 slightly more common than incompatibilities resulting from three or four interacting alleles and
272 that interactions above fourth order made up 2.79 percent of all incompatibilities. However, we note
273 that the frequencies of incompatibility order varied depending on the ancestral population.

274 The pattern of complex genetic interactions provides insights on the distribution of reproductive
275 isolation. Based on the independent assortment mechanism in our model—and assuming that
276 multiple incompatibilities rarely occurred between two parental GRNs—we conclude that hybrid
277 incompatibilities quite often involved higher order interactions, which did not arise as a result
278 of selection, but simply were an expected consequence of GRNs being high order (*Appendix 1*).
279 Further, the discrete characteristic of hybrid incompatibilities led to a higher likelihood at certain
280 RI levels. The band structure in *Figure 5a* agrees with this prediction (*Appendix 1*), which suggests
281 that reproductive barriers are strongly influenced by the concealed hybrid incompatibilities and are
282 coupled with the genetic interaction pattern shown in *Figure 5b*.

283 **Early Divergence between Lineages was Critical for Reproductive Barriers to Emerge**

284 To further study the emergence of reproductive barriers in our model, we investigated the relative
285 importance of various evolutionary forces in generating the observed patterns of RI. In particular,
286 were the barriers attributed to selection pressure, random genetic drift, or both? We designed
287 two “control scenarios” that were based upon the previously simulated model, but contained
288 modifications to remove the effects of either selection or drift. Comparing the strength and pattern
289 of RI resulting from the two control scenarios, i.e., the removal of drift or selection, to the original
290 GRN dynamics, which contain both evolutionary forces, provides an assessment of the removed
291 component’s role in shaping the observed pattern of RI.

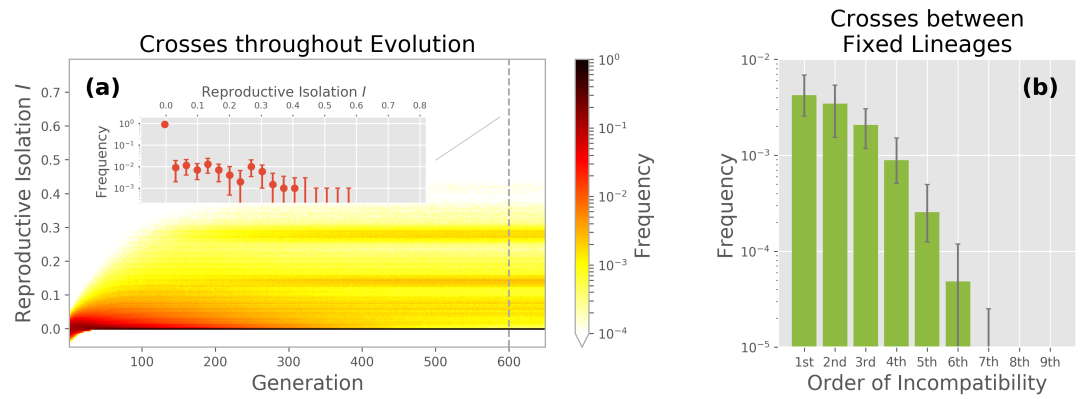


Figure 5. Reproductive barriers arose rapidly between allopatric populations. (a, Inset) Distribution of reproductive isolation between pairs of fixed lineages. A non-negligible fraction of crosses led to positive reproductive isolation, which reflects the occurrence of inviable hybrids and indicates reproductive barriers between fixed lineages. **(a)** We crossed allopatric populations at every generation during GRN evolution and stacked the RI distributions into a heat map. A vertical slice in this heat map represents the RI distribution at a given time, similar to the inset, but where the color shows the mean frequency for each bin. The growing level of positive RI indicates that reproductive barriers arose at the early stage of evolution. **(b)** Frequency that incompatibilities with various order were observed among hybrids between fixed lineages. We see that the order of incompatibilities included a broad range and that the simple pairwise interaction did not significantly dominate over more complex incompatibilities. Moreover, hybrid incompatibilities are consistent with the clustered level of RI and hence sheds light on the observed RI distribution (*Appendix 1*). In both the inset and panel (b), the plots show the statistic of the distribution among multiple groups of allopatric populations, specifically the median frequency and the 95% confidence interval.

292 Removing the effect of natural selection is straightforward to simulate. In this control scenario,
 293 populations simply evolve in a selectively neutral environment where all GRNs are viable. Thus, all
 294 individuals survived and genetic drift became the only remaining evolutionary force. Of course,
 295 this neutrality concurrently made the RI metric ill-defined. We avoided this issue in the crossing
 296 experiments to calculate RI by placing the parental populations under the same non-neutral
 297 environment in the original model, so the hybrids would be generated from survivors subjected to
 298 selection pressure. The reproductive isolation metric could then be computed with respect to the
 299 non-neutral environment. This ensures comparability between the model and the “no selection”
 300 control scenario since the survivability of hybrids was evaluated under the same environment and
 301 was not biased by the otherwise inviable parents.

302 **Figure 6a** shows the contrast of barriers observed in the original GRN evolution model (red) and
 303 in the scenario with no selection (blue). We traced the leading reproductive isolation over time,
 304 defined as the 99th percentile of the RI distribution, which is a sufficient indicator of reproductive
 305 barriers between lineages. We discovered that in both the model and the control scenario, the
 306 leading RI I^* increased and then saturated. Furthermore, the growth in I^* decelerated after a similar
 307 number of generations in both scenarios. That RI occurs at a higher level in the control experiment
 308 indicates that selection did not “cause” the fixation of barriers between allopatric populations,
 309 but instead suggests that selection was actually limiting chances for incompatibilities to occur
 310 in hybrids. We hypothesize that—although restricted as compared to drift—selection operating
 311 on incompatibilities likely induced the observed disconnect between viability and fitness seen in
 312 **Figure 4**.

313 We next turned to the contribution of genetic drift to the emergence of reproductive barriers.
 314 The control scenario, however, was less straightforward due to technical difficulties associated with
 315 directly removing random genetic drift from the model. Neither abandoning sexual reproduction
 316 nor simulating an infinite population would result in non-trivial and/or computationally tractable
 317 GRN evolution. Alternatively, we designed a control scenario where the evolutionary influence

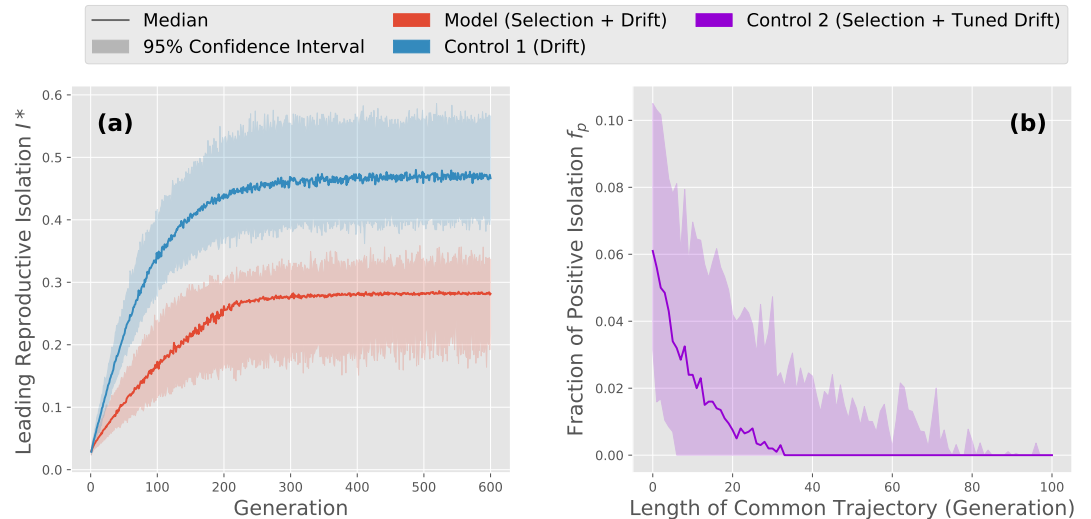


Figure 6. Early divergence of evolutionary trajectories between lineages was necessary for reproductive barriers to arise. Here we compare a statistic, termed leading reproductive isolation I^* (99th percentile of the RI distribution), measuring the degree of reproductive barrier in the original model and two designed control scenarios. Control scenarios were simulated with the same group of ancestral populations as the model, where lineages were then crossed to generate hybrids. **(a)** Leading reproductive isolation I^* among allopatric populations over time, where positive values indicate the existence of reproductive barriers. We plot the original model in red and the control scenario with a neutral environment in blue. The increasing and larger I^* uncovered in the control scenario implies that reproductive barriers were still observed when the selection forces were silenced. **(b)** Long-term fraction of positive RI f_p when the influence of random genetic drift was tuned. We simulated the evolution of lineages, but first confine them to a common trajectory of length L , which was realized by evolving a single population from the ancestors for L generations, and then simulated allopatric evolution from this now less diverse ancestral population. The original model corresponds to the case where $L = 0$, and for any positive L the effect of drift were lessened. We obtained the f_p metric when lineages evolved for 600 generations, where $f_p = 0$ suggests no barriers among populations. That f_p decreased with L to 0 shows that reducing the effect of drift diminished reproductive barriers. As a result, it implies the criticality of divergence among evolutionary trajectories for barriers to emerge.

318 of drift could be tuned and limited. Genetic drift results in stochasticity and causes populations
319 to experience diverse trajectories. On the other side of the coin, if two lineages show similar
320 evolutionary trajectories, one would say that drift effectively leads to less divergence between them.
321 We restricted the influence of genetic drift by first confining lineages in a common trajectory for L
322 generations, and then freed the populations and let them evolve independently, i.e., in allopatry.
323 Varying the length of the common trajectory L tunes the overall similarity among lineages. L hence
324 quantitatively reflects the strength of genetic drift.

325 **Figure 6b** demonstrates the long-term fraction of positive reproductive isolation introduced
326 in *Methods*, termed f_p , as we varied the length of the common trajectory. Despite substantial
327 variation in f_p in the original model, which corresponds to the case where $L = 0$, a decline of
328 f_p was uncovered as early evolutionary confinement was extended. We discovered 50% of the
329 experiments showed a zero f_p in the after lineages were evolved together for 40 generations, and as
330 the length of common trajectory exceeded 80 generations positive reproductive isolation was hardly
331 found between lineages. More importantly, **Figure 6b** suggests that as the evolutionary influence
332 of genetic drift was mitigated, RI was weakened and eventually vanished. Namely, restricting
333 early divergence among populations due to genetic drift diminished reproductive barriers. This
334 control scenario consequently suggests that, instead of the selection pressure, divergence between
335 lineages, coupled with high diversity in the ancestral population, is critical for reproductive barriers
336 to arise.

337 **Intra-lineage Incompatibilities were Eliminated Stochastically While Inter-lineage** 338 **Incompatibilities Persisted and Led to Reproductive Barriers**

339 To better understand how reproductive barriers might be removed within a lineage, but persist
340 between lineages, we computed two quantities from the underlying genetic pool. First, the size
341 of the genetic pool, which determines how many possible genotypes a population contains. This
342 measure captures the potential genetic diversity in the population. Second, we count the number
343 potential incompatibilities in the underlying genetic pool, which are lethal allelic combinations
344 that could potentially be realized in the next generation. These incompatibilities compose the
345 source of inviable offspring and RI between allopatric populations. However, because even for
346 small GRNs searching for all possible incompatibilities quickly becomes computationally intractable,
347 we developed a novel algorithm (summarized in *Methods*) to compute their number in the genetic
348 pool.

349 Because our model does not contain mutation, one would expect the size of the underlying
350 genetic pool to decline in our simulated gene network evolution. Any allele in an individual was
351 inherited from its parents, and thus it must appear in the parental generation as well. Additionally,
352 a parental allele might not persist in the offspring for two possibilities: either it was not transmitted
353 because of finite population size of the progeny generation and the stochasticity during sexual
354 reproduction, i.e. drift, or it formed a lethal pathway along with other inherited alleles which made
355 the offspring inviable, i.e. selection.

356 **Figure 7a** demonstrates the size of genetic pool over time, where we compare simulations in the
357 original model (red) and in the control scenario without selection pressure, i.e., only genetic drift
358 will reduce the size of the genetic pool (blue). A rapid decline of genotypic diversity was witnessed
359 under both models. More intriguingly, little difference was found between the GRN evolution model
360 and the control scenario under a neutral environment. The two median curves nearly overlaps, and
361 for any given generation, the pool size in the original model was not significantly smaller than the
362 control counterpart. Therefore, we find additional support for our earlier finding that although both
363 natural selection and random genetic drift decreased genotypic diversity, drift was the dominant
364 driving force. However, while the effect of drift reduced diversity within a lineage, it increased the
365 divergence among lineages.

366 **Figure 7b** shows the number of potential incompatibilities within a lineage's underlying genetic
367 pool (orange). We found that the amount of incompatibilities embedded in a population also

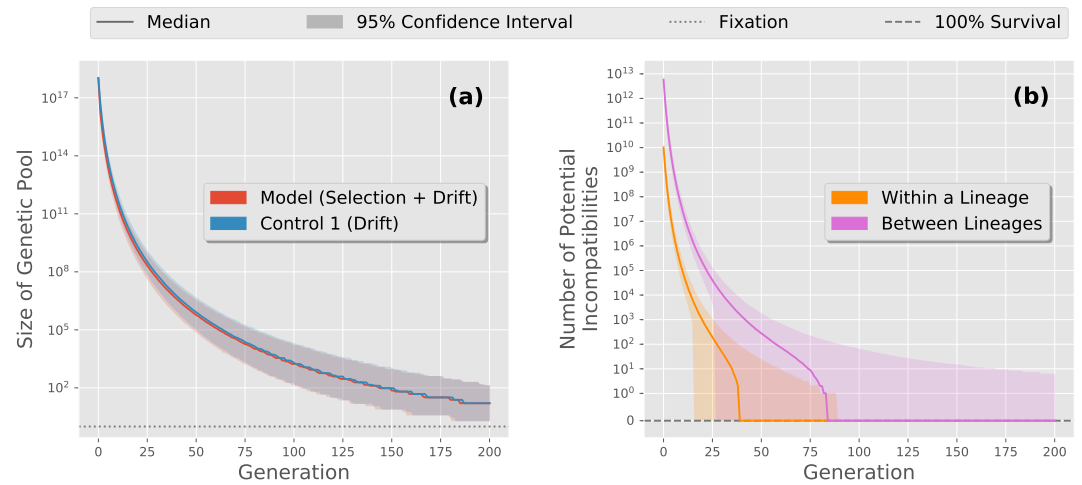


Figure 7. The underlying genetic pool lost alleles and eliminated potential incompatibilities within allopatric populations, whereas inter-lineage incompatibilities persisted. (a) Size of the underlying genetic pool for each generation, where we plot the original model in red along with the no selection control scenario in blue. Both cases show a similar reduction in the genetic pool. The similarity of these curves suggests that the continual losses of allelic diversity within a lineage was dominated by random genetic drift. **(b)** Number of potential intra-lineage (orange) and inter-lineage (pink) incompatibilities for each generation in the original model. We found that the number of potential incompatibilities also decreased as GRNs evolved, which is explained by the reduced allelic diversity in the genetic background. The vanishing intra-lineage incompatibilities implies disappearing sources of inviable hybrids, and it provides a mechanistic understanding of how a genotypically rich populations adapted to the imposed environment. Contrarily, the intra-lineage incompatibilities remained during GRN evolution. It was the persistent potential incompatibilities between allopatric populations that led to evident reproductive barriers.

Figure 7-Figure supplement 1. Inter-lineage incompatibilities were sustained throughout GRN evolution.

368 decreased over time. This phenomenon is understood by the continual loss of allelic diversity,
 369 since removing an allele from the underlying pool always restricts the possibilities to form a lethal
 370 pathway in the GRN. Furthermore, the number of potential incompatibilities fell rapidly until no
 371 potential incompatibilities remained. The elimination of potential incompatibilities illuminates how
 372 a population adapted to the imposed environment when GRNs evolved, as shown in *Figure 3a*.
 373 Random genetic drift drove the loss of a lineage's genotypic diversity, and along with the guidance of
 374 selection, it eliminated probable lethal pathways in the genetic background. Once all the potential
 375 incompatibilities were eliminated, no source of inviable offspring existed and consequently the
 376 population reached 100% survival. Again, this result supports our earlier finding that natural
 377 selection was operating against incompatibilities within a lineage, but that drift was nevertheless
 378 the dominate force in structuring incompatibilities between lineages.

379 Finally, we investigated incompatibilities between underlying pools of lineages, which we call
 380 the "inter-lineage" incompatibilities, as compared to potential lethal allelic combinations within
 381 a population termed "intra-lineage" incompatibilities. *Figure 7b* presents the number of inter-
 382 lineage incompatibilities over generations (pink). We observed more incompatibilities between
 383 allopatric populations than those within a population, i.e., sympatric RI, and similarly their amount
 384 dropped as allelic diversity decreased. In contrast, inter-lineage incompatibilities were removed
 385 at a slower pace compared to intra-lineage incompatibilities. The sustained confidence interval
 386 further suggests that some inter-lineage incompatibilities persisted, which was also the case after
 387 populations reached fixation (*Figure 7-Figure Supplement 1*). The persistence of these potential
 388 incompatibilities qualitatively explain the inviable hybrids revealed after GRN evolution. In spite
 389 of lineages adapting to the same imposed environment, hybridization can "resurrect" a lethal
 390 combination of alleles, which was eliminated in either lineages yet remained in their joint genetic
 391 background. This explanation also supports the stronger barriers uncovered in the neutrally

392 evolving control in **Figure 6a**, since inter-lineage incompatibilities would be more persistent without
393 the constant selection pressure (**Figure 7–Figure Supplement 1**).

394 Discussion

395 In this work, we propose a path-oriented construction of GRNs where alleles are labeled and
396 presented by their functionality. The pathway framework brings a natural perception of GRNs
397 considering how a genotype can give rise to a phenotype, and it allows us to apply network science
398 analyses to study the process of speciation. We simulated the generational dynamics of gene
399 networks via a model incorporating natural selection, segregation and random sampling. With
400 the presumption of ancestral genetic variants, a population adapted to the imposed environment
401 and fixed a single GRN, whereas parallel allopatric populations resulted in alternative regulatory
402 structures. More importantly, we discovered reproductive barriers that arose rapidly among
403 allopatric lineages even under the same selection pressure.

404 We also provide a mechanistic illustration of how reproductive isolation emerged as GRNs
405 evolved. Early evolutionary divergence of lineages, particularly the way they lost accessible alleles
406 in their genetic background, established the base of reproductive barriers. Despite that allopatric
407 populations adapted to the imposed environment whose genetic background no longer contained
408 lethal allelic combinations, potential incompatibilities could persist in the joint background of two
409 parallel lineages. Interbreeding them might therefore resurrect previous removed incompatibilities
410 and led to inviable hybrids.

411 The persistence of inter-lineage incompatibilities implies co-occurrence of many GRNs with
412 negative reproductive interaction under the same selection force. This “functionally degenerate”
413 characteristic of GRNs reflects the concept of genetic redundancy (*Nowak et al., 1997; Láruson*
414 *et al., 2020*), and it resonates with earlier studies that suggested alternative regulatory structures
415 to achieve the same phenotype (*True and Haag, 2001; Wagner and Wright, 2007; Schiffman and*
416 *Ralph, 2018*). Our pathway framework illustrates why degenerate genotypes can naturally arise.
417 Once the alleles are presented as functional pathways connecting a underlying group of proteins,
418 the conjunction between genetic factors and physiological traits is no longer a bipartite mapping;
419 the phenotype, as the collective chemical status of proteins, is a convolution of active signals
420 and external stimuli propagating on the network consisting of genetic pathways. The pathway
421 configuration that satisfies an acknowledged environmental input and phenotypic output is, as
422 a result, not unique. One could find numerous functionally degenerate gene network structures
423 fulfilling the input-output pair, as what **Figure 4** demonstrates, whereas mixing edges between two
424 GRNs possibly leads to a fatal pathway and hence an inviable offspring. Therefore, we evidence that
425 the pathway framework underlines the role of GRNs in speciation processes through the innovative
426 edge-and-node interpretation between genotypes and phenotypes.

427 Our minimal model of GRN evolution encapsulates selection through binary viability, which is
428 essentially a special of holey adaptive landscapes (*Gavrilets, 1997*). *Gavrilets and Gravner (1997)*
429 introduced a multi-locus model where each genotype was independently assigned to one of
430 the two fitness level. The study suggested that reproductive isolation could arise from the high
431 dimensionality of the genotype space, which bypassed and connected seemingly disjoint genotypic
432 regions. In a similar spirit, our model further ties the high dimensionality of genotypes to complex
433 genetic interactions; under the pathway framework, inviability originates at the mechanism of
434 hybrid incompatibilities, i.e., allelic combinations that form lethal pathways in a GRN. The pathway
435 framework also features flexibility, and in future works it can be combined with other fitness
436 landscapes that have been investigated in the speciation literature. For example, *Barton (2001)*
437 demonstrated that stabilizing selection can generate reproductive isolation, and the pathway
438 framework can be easily embedded into such a continuous fitness landscape.

439 Our work endorses the latent connection between speciation processes and ancestral genetic
440 variation. Ancient polymorphisms not only confound inference of evolutionary processes that
441 can drive genomic divergence (*Guerrero and Hahn, 2017*), but they have also been hinted as a

442 potentially good substrate for rapid speciation through the combinatorial mechanism (*Marques*
443 *et al.*, 2019). In particular *Marques et al.* reviewed that old genetic variants had undergone selection
444 and thus likely to be beneficial, they would have higher allele frequency than *de-novo* mutations, and
445 they could enrich large-effect haplotypes and more. Alternatively, we demonstrate that stochasticity
446 of losing accessible pathways in GRNs relatively thrived selected functional regulatory structures
447 among ancestral polymorphisms. Segregating these regulatory structures may notwithstanding
448 upraise deadly pathways. Our pathway framework hence adds theoretical supports to findings of
449 substantial inheritable polymorphism in hybrid incompatibilities, as reviewed in *Cutter (2012)*. We
450 suggest to consider evolution of regulatory pathways as a parallel mechanism with which ancestral
451 genetic variation can facilitate appearance of new species.

452 In principle, any group of ancestral polymorphisms that encodes a lethal regulatory pathway
453 induces a non-zero chance of reproductive isolation. We numerically assessed the strength of re-
454 productive barriers reflecting on the tuned ancestral variation (*Appendix 2*). For finite-size allopatric
455 populations, there appeared a critical amount of variants to observe evident barriers. Further theo-
456 retical efforts are required to quantitatively comprehend the strength of barriers and its relation
457 with the extent of ancestral variation. First, one needs more advanced analyses than *Appendix 1* to
458 evaluate the survival probability of hybrids given multiple incompatibilities embedded in parental
459 GRNs. Second, the likelihood that a certain incompatibility lies between two parental GRNs depends
460 on the balanced distribution of regulatory structures, for instance *Figure 4* as the case at fixation.
461 The skewed patterns of fixed GRNs sketches that some regulatory structures are more favorable
462 than others under evolution. Understanding the balance between gene regulation is necessary to
463 model the dynamics of hybrid incompatibilities.

464 **Methods**

465 **Numerical Simulations**

466 **General Schema and Assumptions**

467 In this work we simulated evolution GRNs in allopatric populations. Throughout evolution, we
468 assumed that individuals had a constant number of loci and thus a fixed number of edges in their
469 GRNs. The underlying set of nodes in GRNs also remained unchanged as we reasoned in *Results*.
470 We further introduced different categories of nodes/proteins to concrete the space of plausible
471 alleles. Some proteins were presumed to only be present with the environmental stimuli, which
472 were not products of any locus; on the other hand, some other proteins were presumed to have
473 mere physiological effects, and thus they were not capable of activating gene expression. We called
474 them source proteins and target proteins respectively. A plausible allele was therefore labeled
475 by a non-target protein that could activate its expression and a non-source protein that would be
476 synthesized. In our simulations we supposed only one source protein and one target protein.

477 We considered a naive model of GRN evolution incorporating natural selection, independent
478 assortment and random genetic drift. The environmental condition was set fixed over time and
479 across populations. We assumed that the environment stimulated presence of one protein and it
480 specified another protein with a lethal effect³. Viability of individuals was presumably equated to
481 the reciprocal binary state of the lethal protein. Hence given the current generation, individuals
482 were selected such that whoever did not possess a pathway from the environmental stimulus to
483 the lethal protein survived and were able to reproduce.

484 The survivors then randomly mated and formed the next generation with independent assort-
485 ment. Here we assumed individuals with haploid-dominant life cycles, where the multicellular
486 haploid stage is evident⁴. Supposed even segregation during meiosis of the diploid zygotes, we
487 modeled the process of independent assortment as follow. Two parental individuals were randomly

³Specifically, they reconciled with the source and the target protein respectively.

⁴During reproduction, specialized haploid cells from two individuals combined and formed a diploid zygote. The zygote experienced meiosis and generated haploid spores, which then developed into multicellular-haploid-stage individuals through mitosis.

488 sampled from the survivors. The set of loci was first randomly partitioned into two groups of equal
489 sizes. The offspring inherited alleles of one group of loci from one of its parents and alleles of the
490 remaining loci from the other parent. Hence half of the edges in the offspring's GRN came from
491 one parent's GRN and the rest was acquired from the other. This procedure was repeated until the
492 next generation had the same constant population size as their predecessors.

493 Simulations and Parameter Setups

494 Here we summarize the two different parameter setups in our simulations:

495 **Setup 1:** We assumed 11 possibly existing proteins in the organism. A generation was composed of
496 100 individuals with 10 loci each. We generated 100 ancestral populations where individuals'
497 GRNs were randomly sampled from all plausible genotypes. For every ancestral population,
498 we in parallel ran 100 simulations from it, which were regarded as lineages evolving in isolated
499 geo-locations.

500 **Setup 2:** We assumed 5 possibly existing proteins in the organism. A generation was composed
501 of 16 individuals with 4 loci each. We generated 10^4 ancestral populations induced from a
502 genetic pool⁵ containing all plausible alleles for each locus. For every ancestral population, we
503 in parallel simulated 10^3 lineages from it.

504 The randomly generated ancestral populations encapsulate our assumption of ancestral genetic
505 variation, which reflect divergence of gene regulation that has been found in empirical studies
506 (*Gould et al., 2018*). Setup 2 aimed to examine how broadly, in terms of fixed GRNs, evolution can
507 explore in all possibilities. Thus it consisted of a larger amount of simulations starting with unbiased
508 ancestral populations that were induced from a maximal genetic pool. If not otherwise specified,
509 simulations shown in Results were run under Setup 1.

510 When we inspected reproductive barriers between allopatric populations by interbreeding them,
511 we first sampled 1000 pairs of lineages and then each generated F_1 1000 hybrids. The survival
512 probability of hybrids can then be obtained for all crosses. The same sampling procedure was also
513 applied when we computed the number inter-lineage potential incompatibilities between pairs of
514 allopatric populations.

515 Metrics of Reproductive Isolation

516 We introduce a quantitative measure of reproductive isolation between lineages which evolved
517 from a common ancestral population. Given a group of lineages and a chosen pair among them,
518 the reproductive isolation between the pair is defined as the relative difference of hybrid survival

$$I = \frac{p_c - p_h}{p_c} \quad (1)$$

519 where p_h is the survival probability of F_1 hybrids, and p_c denotes the average of survival probabilities
520 of all lineages' next generation. A positive value of reproductive isolation I implies that the hybrids
521 have less survivability than the expectation of the offspring. In the extreme case where no hybrid
522 lives, $I = 1$. It therefore serves as an indicator of reproductive barriers between two lineages.

523 Strengths of reproductive barriers among the group of lineages are described through a distribu-
524 tion of reproductive isolation, which can be obtained by sampling pairs of lineages and computing
525 their reproductive isolation I . We further introduce two indicators for the existence of reproductive
526 barriers. A quantity named leading reproductive isolation I^* is defined as the 99th percentile of the
527 reproductive isolation distribution. It signals that there is one percent of crosses with reproductive
528 isolation equal or larger than I^* . We would also like to raise a caveat that $I^* > 0$ is sufficient for the
529 existence of reproduction barriers but not a necessary condition, due to the possibility of positive
530 I in the distribution even if $I^* \leq 0$. The leading reproductive isolation metric hence summarizes
531 a high level of reproductive barriers that can be found among the lineages. On the other hand,

⁵We refer a population induced from a genetic pool to a sample among all possible populations that own the same underlying genetic pool.

532 the fraction of positivity in the reproductive isolation distribution serves as a necessity indicator
533 for reproductive barriers, which we denote as f_p . The zero-value of f_p implies that none of the
534 crosses generate inviable hybrids more than the anticipation of the offspring and thus the absence
535 of reproductive barriers. Contrarily, a positive f_p does not satisfy existence of barriers considering
536 small reproductive isolation subject to noise. These two indicators are beneficial for us to identify
537 the responsible part of the model to the observed evolutionary consequences.

538 **Potential Incompatibilities within and between Genetic Pools**

539 An intra-lineage incompatibility is a group of alleles in its genetic pool, each of a unique locus, that
540 generates a lethal pathway. In our model those incompatibilities are the only source of inviability,
541 and hence the number of potential incompatibilities provides information about reproductive
542 barriers. Nevertheless, counting the number of potential incompatibilities within a genetic pool
543 through a brute-force manner is computationally intractable. Here we suggest a relatively efficient
544 algorithm when the total number of loci is small. Our strategy is to turn the task into solving a graph
545 problem. The genetic pool can be transformed to an edge-colored network where nodes once more
546 represent possibly existing proteins in the organism. The edges correspond to available alleles
547 in the pool, which are colored by their according loci. A potential incompatibility then becomes
548 a simple path from an environmental input signal to a lethal protein node, with an additional
549 constrain that no edges on the path have the same color. We call such a path an edge-colorful
550 simple path (ECSP).

551 The proposed algorithm, as demonstrated in **Appendix 3** Algorithm 1, counts the number of
552 ECSPs from the source nodes to the targets nodes by having agents propagate on the edge-colored
553 network iteratively. An agents is capable of keeping information of the trajectory, including its
554 current position on the network, the colors of edges it has traversed and the nodes that it has
555 visited⁶. Initially we deploy one agent on each source node. At every iteration, each agent is
556 substituted by all of its possible successors who are a hop away, such that the hop along with the
557 agent's memory obeys an edge-colorful simple path. Those successors can be deduced from the
558 agent's trajectory information as shown in **Appendix 3** Algorithm 2. The cautiously-designed rule of
559 agent propagation guarantees that the total number of agents locating on the target nodes at the
560 n th iteration equals to the number of the desired ECSPs of length n . Moreover, since the order of
561 an potential incompatibility is bounded above by the number of genes in the organism, iterations
562 as many as the amount of edge colors in the network are sufficient to obtain a computationally
563 feasible count of all potential incompatibilities. The efficiency of the algorithm can be further
564 improved by, instead of keeping track of numerous agents, monitoring the distribution of agent
565 states over iterations.

566 The same algorithm can be applied to count the number of inter-lineage incompatibilities
567 as well. In this case the underlying genetic pools of both lineages are transformed into a single
568 edge-colored network, whose edges then consist of alleles in the two pools and are again colored
569 by their according loci. A ECSP on this composite network either only traverses through edges
570 from one of the genetic pools, or it contains alleles from the two different pools. These two
571 scenarios correspond to a incompatibility within and between genetic pools respectively. Therefore,
572 by counting the number of ECSPs on the composite network, and subtracting by the number of
573 potential incompatibilities within the two genetic pools separately, we can compute the number of
574 incompatibilities between the two underlying genetic pools.

575 **References**

576 **Barton NH.** The role of hybridization in evolution. *Molecular ecology*. 2001; 10(3):551–568.

577 **Bateson W.** Heredity and variation in modern lights. *Darwin and modern science*. 1909; .

⁶In Algorithm 1, the NEW-AGENT procedure creates an agent instance given its position, visited colors and nodes accordingly. This trajectory information is also accessible fields of the agent instance.

- 578 **Bikard D**, Patel D, Le Metté C, Giorgi V, Camilleri C, Bennett MJ, Loudet O. Divergent evolution of duplicate genes
579 leads to genetic incompatibilities within *A. thaliana*. *Science*. 2009; 323(5914):623–626.
- 580 **Boyle EA**, Li YI, Pritchard JK. An Expanded View of Complex Traits: From Polygenic to Omnigenic. *Cell*.
581 2017; 169(7):1177 – 1186. <http://www.sciencedirect.com/science/article/pii/S0092867417306293>, doi:
582 <https://doi.org/10.1016/j.cell.2017.05.038>.
- 583 **Brideau NJ**, Flores HA, Wang J, Maheshwari S, Wang X, Barbash DA. Two Dobzhansky-Muller genes interact to
584 cause hybrid lethality in *Drosophila*. *science*. 2006; 314(5803):1292–1295.
- 585 **Chae E**, Bomblies K, Kim ST, Karelina D, Zaidem M, Ossowski S, Martín-Pizarro C, Laitinen RE, Rowan
586 B, Tenenboim H, Lechner S, Demar M, Habring-Müller A, Lanz C, Rättsch G, Weigel D. Species-wide
587 Genetic Incompatibility Analysis Identifies Immune Genes as Hot Spots of Deleterious Epistasis. *Cell*.
588 2014; 159(6):1341 – 1351. <http://www.sciencedirect.com/science/article/pii/S0092867414013762>, doi:
589 <https://doi.org/10.1016/j.cell.2014.10.049>.
- 590 **Coyne JA**, Allen Orr H. The evolutionary genetics of speciation. *Philosophical Transactions of the Royal Society*
591 *of London Series B: Biological Sciences*. 1998; 353(1366):287–305.
- 592 **Cutter AD**. The polymorphic prelude to Bateson–Dobzhansky–Muller incompatibilities. *Trends in ecology &*
593 *evolution*. 2012; 27(4):209–218.
- 594 **Davidich M**, Bornholdt S. The transition from differential equations to Boolean networks: A case study in
595 simplifying a regulatory network model. *Journal of Theoretical Biology*. 2008; 255(3):269 – 277. <http://www.sciencedirect.com/science/article/pii/S0022519308003652>, doi: <https://doi.org/10.1016/j.jtbi.2008.07.020>.
- 597 **Davies B**, Hatton E, Altemose N, Hussin JG, Pratto F, Zhang G, Hinch AG, Moralli D, Biggs D, Diaz R, et al.
598 Re-engineering the zinc fingers of PRDM9 reverses hybrid sterility in mice. *Nature*. 2016; 530(7589):171–176.
- 599 **De Bruijn NG**. A combinatorial problem. In: *Proc. Koninklijke Nederlandse Academie van Wetenschappen*, vol. 49;
600 1946. p. 758–764.
- 601 **Dobzhansky T**. Studies on hybrid sterility. II. Localization of sterility factors in *Drosophila pseudoobscura*
602 hybrids. *Genetics*. 1936; 21(2):113.
- 603 **Duranton M**, Allal F, Valière S, Bouchez O, Bonhomme F, Gagnaire PA. The contribution of ancient admixture to
604 reproductive isolation between European sea bass lineages. *BioRxiv*. 2019; p. 641829.
- 605 **Gavrilets S**. Evolution and speciation on holey adaptive landscapes. *Trends in ecology & evolution*. 1997;
606 12(8):307–312.
- 607 **Gavrilets S**, Gravner J. Percolation on the fitness hypercube and the evolution of reproductive isolation. *Journal*
608 *of theoretical biology*. 1997; 184(1):51–64.
- 609 **Gould BA**, Chen Y, Lowry DB. Gene regulatory divergence between locally adapted ecotypes in their native
610 habitats. *Molecular Ecology*. 2018; 0(0). <https://onlinelibrary.wiley.com/doi/abs/10.1111/mec.14852>, doi:
611 [10.1111/mec.14852](https://doi.org/10.1111/mec.14852).
- 612 **Guerrero RF**, Hahn MW. Speciation as a sieve for ancestral polymorphism. *Molecular ecology*. 2017; 26(20):5362–
613 5368.
- 614 **Johnson NA**, Porter AH. Rapid speciation via parallel, directional selection on regulatory genetic pathways.
615 *Journal of Theoretical Biology*. 2000; 205(4):527–542.
- 616 **Kalirad A**, Azevedo RBR. Spiraling Complexity: A Test of the Snowball Effect in a Computational Model of RNA
617 Folding. *Genetics*. 2017; 206(1):377–388. <http://www.genetics.org/content/206/1/377>, doi: [10.1534/genetics.116.196030](https://doi.org/10.1534/genetics.116.196030).
- 619 **Kuzmin E**, VanderSluis B, Wang W, Tan G, Deshpande R, Chen Y, Usaj M, Balint A, Mattiazzi Usaj M, van Leeuwen
620 J, Koch EN, Pons C, Dagilis AJ, Pryszyk M, Wang JZY, Hanchard J, Riggi M, Xu K, Heydari H, San Luis BJ, et al.
621 Systematic analysis of complex genetic interactions. *Science*. 2018; 360(6386). <http://science.sciencemag.org/content/360/6386/eaao1729>, doi: [10.1126/science.aao1729](https://doi.org/10.1126/science.aao1729).
- 622
- 623 **Langfelder P**, Horvath S. WGCNA: an R package for weighted correlation network analysis. *BMC bioinformatics*.
624 2008; 9(1):559.

- 625 **Láruson ÁJ**, Yeaman S, Lotterhos KE. The Importance of Genetic Redundancy in Evolution. *Trends in Ecology &*
626 *Evolution*. 2020; .
- 627 **Livingstone K**, Olofsson P, Cochran G, Dagilis A, MacPherson K, Seitz KA. A stochastic model for the development
628 of Bateson–Dobzhansky–Muller incompatibilities that incorporates protein interaction networks. *Mathemati-*
629 *cal Biosciences*. 2012; 238(1):49 – 53. <http://www.sciencedirect.com/science/article/pii/S0025556412000491>,
630 doi: <https://doi.org/10.1016/j.mbs.2012.03.006>.
- 631 **Marques DA**, Meier JI, Seehausen O. A combinatorial view on speciation and adaptive radiation. *Trends in*
632 *ecology & evolution*. 2019; .
- 633 **Meier JI**, Marques DA, Mwaiko S, Wagner CE, Excoffier L, Seehausen O. Ancient hybridization fuels rapid cichlid
634 fish adaptive radiations. *Nature communications*. 2017; 8:14363.
- 635 **Muller H**. Isolating mechanisms, evolution, and temperature. In: *Biol. Symp.*, vol. 6; 1942. p. 71–125.
- 636 **Nelson TC**, Cresko WA. Ancient genomic variation underlies repeated ecological adaptation in young stickleback
637 populations. *Evolution Letters*. 2018; 2(1):9–21.
- 638 **Nowak MA**, Boerlijst MC, Cooke J, Smith JM. Evolution of genetic redundancy. *Nature*. 1997; 388(6638):167–171.
- 639 **Orr HA**. The population genetics of speciation: the evolution of hybrid incompatibilities. *Genetics*. 1995;
640 139(4):1805–1813. <http://www.genetics.org/content/139/4/1805>.
- 641 **Palmer ME**, Feldman MW. DYNAMICS OF HYBRID INCOMPATIBILITY IN GENE NETWORKS IN A CONSTANT
642 ENVIRONMENT. *Evolution*. 2009; 63(2):418–431. [https://onlinelibrary.wiley.com/doi/abs/10.1111/j.1558-5646.](https://onlinelibrary.wiley.com/doi/abs/10.1111/j.1558-5646.2008.00577.x)
643 [2008.00577.x](https://onlinelibrary.wiley.com/doi/abs/10.1111/j.1558-5646.2008.00577.x), doi: [10.1111/j.1558-5646.2008.00577.x](https://doi.org/10.1111/j.1558-5646.2008.00577.x).
- 644 **Powell DL**, García-Olazábal M, Keegan M, Reilly P, Du K, Díaz-Loyo AP, Banerjee S, Blakkan D, Reich D, Andolfatto
645 P, et al. Natural hybridization reveals incompatible alleles that cause melanoma in swordtail fish. *Science*.
646 2020; 368(6492):731–736.
- 647 **Rieseberg LH**, Sinervo B, Linder CR, Ungerer MC, Arias DM. Role of gene interactions in hybrid speciation:
648 evidence from ancient and experimental hybrids. *Science*. 1996; 272(5262):741–745.
- 649 **Satokangas I**, Martin S, Helanterä H, Saramäki J, Kulmuni J. Multi-locus interactions and the build-up of
650 reproductive isolation. *arXiv preprint arXiv:200513790*. 2020; .
- 651 **Schiffman JS**, Ralph PL. System drift and speciation. *bioRxiv*. 2018; [https://www.biorxiv.org/content/early/2018/](https://www.biorxiv.org/content/early/2018/01/26/231209)
652 [01/26/231209](https://www.biorxiv.org/content/early/2018/01/26/231209), doi: [10.1101/231209](https://doi.org/10.1101/231209).
- 653 **Schlitt T**, Brazma A. Current approaches to gene regulatory network modelling. *BMC bioinformatics*. 2007;
654 8(S6):S9.
- 655 **Schluter D**. Evidence for Ecological Speciation and Its Alternative. *Science*. 2009; 323(5915):737–741. [http://](http://science.sciencemag.org/content/323/5915/737)
656 science.sciencemag.org/content/323/5915/737, doi: [10.1126/science.1160006](https://doi.org/10.1126/science.1160006).
- 657 **Sicard A**, Kappel C, Josephs EB, Lee YW, Marona C, Stinchcombe JR, Wright SI, Lenhard M. Divergent sorting of
658 a balanced ancestral polymorphism underlies the establishment of gene-flow barriers in *Capsella*. *Nature*
659 *communications*. 2015; 6:7960.
- 660 **Tong AHY**, Lesage G, Bader GD, Ding H, Xu H, Xin X, Young J, Berriz GF, Brost RL, Chang M, et al. Global mapping
661 of the yeast genetic interaction network. *science*. 2004; 303(5659):808–813.
- 662 **True JR**, Haag ES. Developmental system drift and flexibility in evolutionary trajectories. *Evolution & develop-*
663 *ment*. 2001; 3(2):109–119.
- 664 **Turner LM**, White MA, Tautz D, Payseur BA. Genomic Networks of Hybrid Sterility. *PLOS Genetics*. 2014 02;
665 10(2):1–23. <https://doi.org/10.1371/journal.pgen.1004162>, doi: [10.1371/journal.pgen.1004162](https://doi.org/10.1371/journal.pgen.1004162).
- 666 **Wagner A**, Wright J. Alternative routes and mutational robustness in complex regulatory networks. *Biosystems*.
667 2007; 88(1-2):163–172.
- 668 **Wang B**, Mojica JP, Perera N, Lee CR, Lovell JT, Sharma A, Adam C, Lipzen A, Barry K, Rokhsar DS, et al. Ancient
669 polymorphisms contribute to genome-wide variation by long-term balancing selection and divergent sorting
670 in *Boechera stricta*. *Genome biology*. 2019; 20(1):126.

- 671 **Wittbrodt J**, Adam D, Malitschek B, Mäueler W, Raulf F, Telling A, Robertson SM, Schartl M. Novel puta-
672 tive receptor tyrosine kinase encoded by the melanoma-inducing Tu locus in Xiphophorus. *Nature*. 1989;
673 341(6241):415–421.
- 674 **Yamamoto E**, Takashi T, Morinaka Y, Lin S, Wu J, Matsumoto T, Kitano H, Matsuoka M, Ashikari M. Gain of
675 deleterious function causes an autoimmune response and Bateson–Dobzhansky–Muller incompatibility in
676 rice. *Molecular Genetics and Genomics*. 2010; 283(4):305–315.

677 Appendix 1

678 Hybrid Inviability against a Single Incompatibility

679 Here we analytically evaluate the probability that a hybrid is inviable presuming that multiple
680 incompatibilities are rarely embedded in two parental gene regulatory networks. In addition,
681 this naive analysis explains the pattern of RI distribution, **Figure 5a** in the main text.

682 Assume that there is only one incompatibility I between the two parental gene networks
683 G_1 and G_2 . For convenience we suppose there are an even number of loci in the organisms,
684 denoted by $2m$, and let the incompatibility I be of order $k - 1$ so it consists of k alleles to
685 form a lethal combination. We also suppose that, among the k alleles in I , k_1 of them come
686 from G_1 and the other k_2 alleles are from G_2 .

687 Following the rule of recombination between haploid GRNs in our model, the hybrid is
688 generated by randomly segregating alleles of m loci from G_1 and then mixing with alleles
689 of the other m loci from G_2 . Hence if $m < k_1$ or $m < k_2$, then there is no chance that the
690 incompatibility I appears in the hybrid. Otherwise, among all plausible segregation, we
691 can compute the number of achievable ways that the k_1 and k_2 alleles from G_1 and G_2
692 respectively are sorted into the hybrid. The probability that the hybrid is inviable due to the
693 only incompatibility I is thus

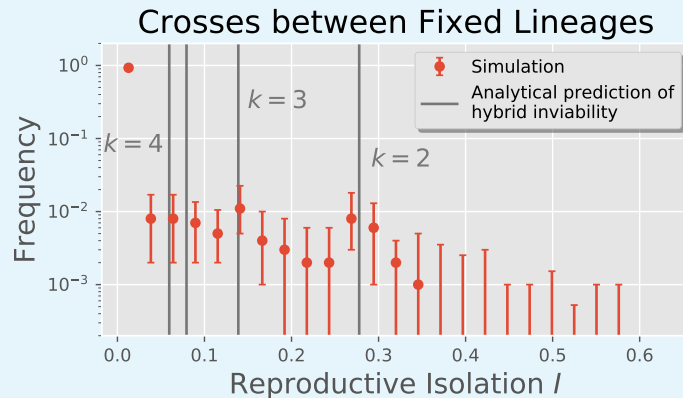
$$694 P(I) = \begin{cases} \frac{\binom{2m-k}{m-k_1}}{\binom{2m}{m}}, & \text{if } k_1, k_2 \leq m \\ 0, & \text{otherwise} \end{cases} \quad (2)$$

697 If we further assume that $m \gg 1$ and $m \gg k$, applying the Stirling's approximation we have
698 an estimate of the hybrid inviability

$$699 P(I) = \frac{m!m!(2m-k)!}{(m-k_1)!(m-k_2)!(2m)!} \approx 2^{-k} \quad (3)$$

702 This plain derivation shows that, should there be only one incompatibility concealing between
703 two parental GRNs, the survivability of a hybrid is predominantly determined by the order of
704 the incompatibility.

705 Here **Figure 1** shows good agreement between our analytical prediction of hybrid invia-
706 bility and the "bulges" from the observed RI distribution. Our simple derivation explains the
707 higher likelihood of certain RI levels relative to their neighboring regions. It also manifests
708 how the discreteness nature of hybrid incompatibilities shapes the RI distribution and that
709 this characteristic has major effects on the strength of reproductive barriers.



710 **Appendix 1 Figure 1.** Comparison between the uncovered RI distribution in our simulations and the
711 predicted hybrid inviability **Equation 2**.
713

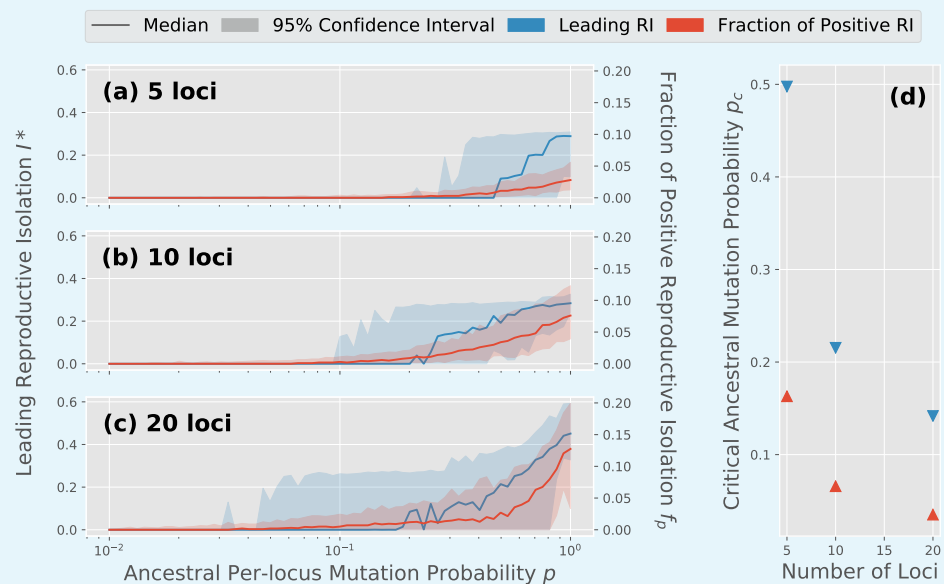
714 Appendix 2

715 Reproductive Barriers and Ancestral Genetic Variation

716 Here we demonstrate our examination on how the extent of ancestral genetic variation
717 influences the appearance and strength of reproductive barriers. To begin with, we designed
718 a pipeline to produce ancestral populations whose amount of genetic variation are tunable.
719 A fixed population was first obtained from our GRN evolution model starting with randomly
720 generated individual GRNs. For every locus, the allele might then mutate into any other
721 possible allele with a per-locus mutation probability p . The resulting population was regarded
722 as the ancestral population, where the mutation probability p became a tunable parameter
723 to assess the degree of ancestral variation.

724 We followed the same methodology to simulate generational dynamics of GRNs and to
725 compute reproductive isolation between allopatric lineages as in the main text. **Figure 1a-c**
726 shows, for different number of loci, the reproductive barriers consequent to the varying
727 ancestral mutation probability p . Here we present two indicators of barriers: the leading RI
728 (blue, left axis) and the fraction of positive RI (red, right axis). On a first glance the simulations
729 evince that, for a organism with a larger number of loci, emergence of barriers only required
730 a smaller ancestral mutation probability yet more apparent barriers were observed.

731 **Figure 1a-c** furthermore suggest some critical level of ancestral variation associated with
732 the constant population size, such that reproductive barriers would hardly appear between
733 lineages evolving from an ancestral population with less polymorphisms. We quantify the
734 critical level of genetic variation through a critical mutation probability p_c : this is the smallest
735 ancestral mutation probability with which a barrier indicator has non-zero median value.
736 Nevertheless, due to the lack of a both sufficient and necessary indicator, we could only
737 estimate the interval that this critical level fell into. The critical level of ancestral variation
738 would be bounded above by p_c for the leading RI (a sufficient indicator of barriers) and
739 bounded below by one for the fraction of positive RI (a necessary indicator of barriers).
740 **Figure 1d** presents the interval estimation that the critical ancestral variation fell into for
741 organisms with different number of loci.



742 **Appendix 2 Figure 1.** Varying the extent ancestral variation and its corresponding strength of
743 reproductive barriers. The GRN evolution was simulated under Setup 1 described in Methods. **(a-c)**
744 Indicators of barriers for 5, 10 and 20 loci. **(d)** Estimation of their critical level of ancestral variation.
745
746

747 Appendix 3

748 Algorithms of Counting Potential Incompatibilities

749 Algorithm 1 COUNT-ECSP

751 **Require:** A set of source nodes S ; a set of target nodes T ; a map I from nodes to their
752 incident outgoing edges; a set of path lengths of interests L .

753 **Ensure:** A map C from L to the number of edge-colorful simple paths from S to T , which
754 are of the corresponding length.

```
755 1:  $C \leftarrow$  an empty map
756 2:  $l_{max} \leftarrow$  the largest element of  $L$ 
757 3:  $A \leftarrow$  an empty list ▷ Initialize agents.
758 4: for all node  $s \in S$  do  $A$ .INSERT(NEW-AGENT( $s, \emptyset, \{s\}$ ))
759 5: end for
760 6: for  $l \leftarrow 1$  to  $l_{max}$  do ▷ Iterate over the number of hops agents have made from the
761 source nodes.
762 7:  $n \leftarrow 0$ 
763 8:  $N \leftarrow$  an empty list ▷ Update the list of agents.
764 9: for all agent  $a \in A$  do
765 10: for all agent  $a' \in$  NEXT-POSSIBILITIES( $a, I$ ) do
766 11:  $N$ .INSERT( $a'$ )
767 12: if  $a'.position \in T$  then  $n \leftarrow n + 1$ 
768 13: end if
769 14: end for
770 15: end for
771 16:  $A \leftarrow N$ 
772 17: if  $l \in L$  then  $C$ .INSERT( $l, n$ ) ▷ Update counting.
773 18: end if
774 19: end for
775 20: return  $C$ 
```

776 Algorithm 2 NEXT-POSSIBILITIES

778 **Require:** An agent a ; a map I from nodes to their incident outgoing edges.

779 **Ensure:** A set P of agents who are of all the possible states that can be reached through a
780 hop from the given agent a , such that

- 781 1. The hop only goes through an edge of a color that has not been visited by the agent.
- 782 2. The position after the hop has not been visited by the agent.

```
783 1:  $P \leftarrow$  an empty set
784 2: for all edge  $e \in I$ .GET( $a$ ) do
785 3: if  $e.color \notin a.colors-visited$  and  $e.target \notin a.nodes-visited$  then
786 4:  $a' \leftarrow$  NEW-AGENT( $e.target, a.colors-visited \cup \{e.color\}, a.nodes-visited \cup \{e.target\}$ )
787 5:  $P$ .INSERT( $a'$ )
788 6: end if
789 7: end for
790 8: return  $P$ 
```

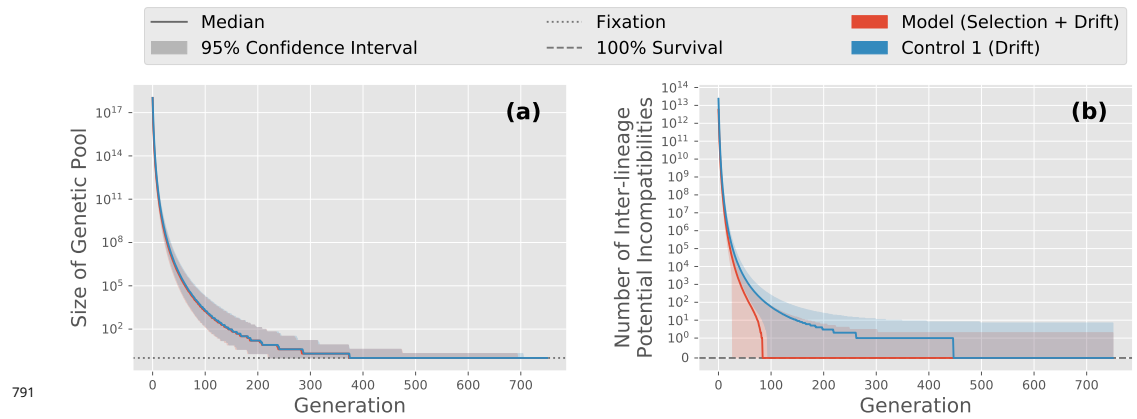


Figure 7-Figure supplement 1. (a) The size the underlying genetic pool continually shrank until there was only one accessible genotype. At this stage a population fixated a single GRN, and no significant difference was found between the model and the control scenario without selection, i.e., drift only. **(b)** In our model, inter-lineage incompatibilities persisted throughout evolution (red), which accounts for the sustained confidence interval of their abundance even after populations reach fixation. Interestingly, in the control scenario where natural selection was silenced, inter-lineage incompatibilities were eliminated at a slower pace. We hypothesize that due to the lack of guidance by selection, inter-lineage incompatibilities only became inaccessible through random genetic drift. This scenario led to fatal allelic combinations that were more persistent than those in the model and hence stronger reproductive barriers were observed.